

Fabrica: Dual-Arm Assembly of General Multi-Part Objects via Integrated Planning and Learning

Yunsheng Tian^{1,†}, Joshua Jacob¹, Yijiang Huang², Jialiang Zhao¹,
Edward Gu¹, Pingchuan Ma¹, Annan Zhang¹, Farhad Javid³, Branden Romero¹,
Sachin Chitta³, Shinjiro Sueda⁴, Hui Li^{3,†}, Wojciech Matusik¹

¹MIT CSAIL, ²ETH Zurich, ³Autodesk Research, ⁴Texas A&M University

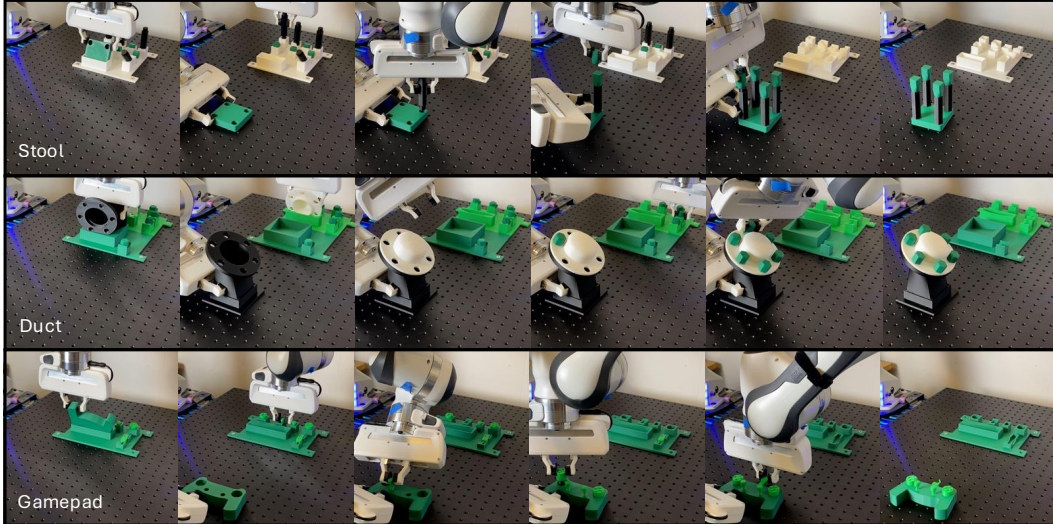


Fig. 1: Our proposed dual-arm robotic system demonstrates adaptive manipulation and assembly capabilities for diverse multi-part objects. The system combines offline task-oriented planning and optimization to address sequencing, grasping, and motion planning for long-horizon assembly tasks. For robust online control, it utilizes guidance from the offline plan to learn assembly skills that generalize effectively across diverse object geometries, assembly paths, and grasp poses.

Abstract: Multi-part assembly poses significant challenges for robots to execute long-horizon, contact-rich manipulation with generalization across complex geometries. We present Fabrica, a dual-arm robotic system capable of end-to-end planning and control for autonomous assembly of general multi-part objects. For planning over long horizons, we develop hierarchies of precedence, sequence, grasp, and motion planning with automated fixture generation, enabling general multi-step assembly on any dual-arm robots. The planner is made efficient through a parallelizable design and is optimized for downstream control stability. For contact-rich assembly steps, we propose a lightweight reinforcement learning framework that trains generalist policies across object geometries, assembly directions, and grasp poses, guided by equivariance and residual actions obtained from the plan. These policies transfer zero-shot to the real world and achieve 80% successful steps. For systematic evaluation, we propose a benchmark suite of multi-part assemblies resembling industrial and daily objects across diverse categories and geometries. By integrating efficient global planning and robust local control, we showcase the first system to achieve complete and generalizable real-world multi-part assembly without domain knowledge or human demonstrations. Project website: fabrica.csail.mit.edu

Keywords: Assembly, Planning, Reinforcement Learning, Benchmark

[†]Correspondence to: yunsheng@mit.edu and hui.xylo.li@autodesk.com

1 Introduction

Multi-part assemblies are prevalent in home and industrial settings. Robotic assembly of multi-part objects presents a longstanding challenge: long-term planning to map CAD models to robot programs and robust control skills to achieve high precision and adaptivity during contact-rich interactions. However, most assembly robots today are programmed manually with specially designed infrastructures, and the program is executed repetitively using a stiff controller. As a result, they take substantial time to adapt to new production demands and are highly sensitive to uncertainties.

Despite recent progress in sim-to-real transfer of contact-rich part insertion skills [1, 2, 3], current robotic systems are still not capable of assembling general multi-part objects. Prior research has primarily focused on two-part, top-down insertion using a single robot arm, but multi-part assembly requires diverse insertion and grasping poses and a bi-manual operation that frequently changes which part to hold to counter-balance the insertion force from the other hand. This presents new challenges to planning and control. First, jointly finding an assembly-hold sequence, physically stable grasps, and collision-free robot motion presents a hybrid (discrete-continuous) optimization problem in a large search space. Second, control policies for part insertion must be robust to mis-alignment and uncertainty, while being able to generalize across a wide range of part geometries.

We tackle these challenges by building a general planning and control system for flexible, dual-arm assembly of multi-part objects, with zero-shot sim-to-real transfer. Our contributions include:

Algorithms: We propose a hierarchical dual-arm planner to plan and optimize the assembly-hold sequence, grasps, and robot motion. For contact-rich steps, we learn generalist reinforcement learning (RL) policies utilizing equivariant representations guided by planned motion to achieve robustness.

Systems: We build a real-world system that can map a CAD assembly model to robot execution that alternates between tracking planned motions and reactive control policies. To our knowledge, this is the first system that autonomously achieves all phases of a multi-part assembly problem: from automatic pickup fixture design, to sequence, grasps, and motion planning, to insertion. Our system is tested on commonly used robotics hardware and can be generalized to different dual-arm robots.

Benchmarks: We design a benchmark suite of 7 multi-part assemblies ranging from 5 to 9 parts, and our system can assemble them robustly in both simulation and real-world system.

2 Related Work

Prior work on multi-part assembly is heavily focused on planning assembly sequences and paths, including geometric reasoning [4], sampling-based motion planners [5, 6, 7], and RL for combinatorial sequence search [8, 9]. Recently, physics-based motion planning [10] has shown success in assembling many complex parts with tight clearances. In addition, realistic kinematic and dynamic constraints have been considered in sequence planning for real-world robot setups [11, 12, 13]. However, planning alone struggles with execution uncertainties, and stability- or efficiency-optimal plans remain underexplored. While robust and efficient robotic systems have been built for tasks like assembling IKEA chairs [14], LEGO blocks [15], and structural elements [16, 17, 18, 19, 20, 21, 22], these are domain-specific and lack generalizability. In contrast, our planner generalizes across diverse multi-part assemblies, employs hierarchical structure and parallelization for efficiency, and explicitly optimizes stability to enhance downstream control robustness.

Even with given assembly plans, executing contact-rich assembly remains challenging due to tight clearances, system uncertainties, and the need for generalization. RL has shown promise in addressing these issues, combining motion planning with policy learning from CAD models or supervised trajectories [23, 24], and leveraging accurate simulations for motion generation and policy training [11, 25]. Sim-to-real transfer [26, 3, 27, 2] and real-world RL [28] have enabled high-precision insertion, while some efforts [29] explore multi-step tasks. However, they all primarily work under simplified settings like top-down insertions and fixed grasps, which are insufficient for multi-part assembly where side-way insertions or tilted grasps are necessary. Imitation learning ap-

proaches [30, 31] support complex multi-step skill learning but lack robustness and generality. While spatial-equivariant techniques have improved generalization in other domains [32, 33, 34, 35, 36], they remain underexplored for assembly. Notably, Seo et al. [37] learn an $SE(3)$ -equivariant gain scheduling policy, but without varying grasps or geometries. Existing benchmarks focus on narrow tasks [38, 39, 40, 41, 42], limiting the evaluation of generalization. In contrast, we demonstrate that combining planning with equivariant generalist policies, for the first time, enables multi-part assembly over diverse geometries, paths, and grasps without any human demonstration.

3 Planning Multi-Step Dual-Arm Assembly

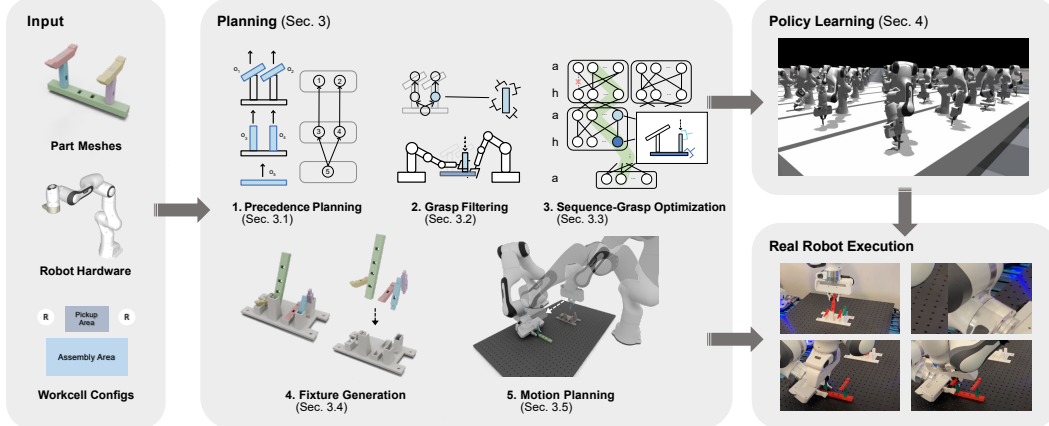


Figure 2: System overview. Fabrica takes part meshes and hardware configurations as inputs. It plans sequences, grasps, fixture designs, and motions through a multi-stage planner, and learns RL policies for all insertion steps, which are deployed together on real robots to complete the assembly.

Given a n -part assembly with parts indexed by $o \in O$, we compute a plan to manipulate all parts from the initial poses p_O^0 to the goal poses $p_O^G \in SE(3)$ under all physical constraints. We focus on sequential, collaborative manipulation that alternates between robot R_a assembling a part and another robot R_h holding a part to stabilize the sub-assembly. Then, we train control policies for precise contact-rich assembly steps. Finally, our system execution alternates between open-loop planned motions and closed-loop reactive policies. Fig. 2 provides an overview of the system.

We formulate planning as optimizing assembly-hold sequences ϕ , grasps σ , and robot motions π :

$$\min_{\phi, \sigma, \pi} E(\Phi_{i=1}^n \vec{f}(\phi_{1:i}, \sigma_{i-1:i}, \pi_i)) \quad \text{s.t.} \quad C_{\text{prec}}(\phi) \leq 0, C_{\text{kin}}(\phi, \sigma, \pi) = 0, C_{\text{col}}(\phi, \sigma, \pi) \leq 0 \quad (1)$$

The sequence $\phi = [o_{a,1}, o_{h,2}, o_{a,2}, \dots, o_{h,n}, o_{a,n}]$ is an ordering of parts to be held (h) and assembled (a), with $\sigma = [g_{a,1}, g_{h,2}, g_{a,2}, \dots, g_{h,n}, g_{a,n}]$ including grasp $g \in SE(3)$ for each step. The robot motion π is divided based on the mode families [43, 44] and skills: $\pi = [\underbrace{\tau_{a,1}^f, \tau_{a,1}^g, \tau_{a,1}^a}_{\pi[a,1]}, \underbrace{\tau_{h,2}^f, \tau_{a,2}^f, \tau_{a,2}^g, \tau_{a,2}^a}_{\pi[h,2]}, \underbrace{\tau_{a,2}^f, \tau_{a,2}^g, \tau_{a,2}^a}_{\pi[a,2]}, \dots]$ where each assembly task $\pi[a, i]$ for R_a contains (1) a

transit motion $\tau_{a,i}^f$ with its hand free, (2) a transfer motion $\tau_{a,i}^g$ grasping an object, and (3) an assembly motion $\tau_{a,i}^a$ for part insertion. A hold task $\pi[h, i]$ only involves a hold transfer motion $\tau_{h,i}^f$. The cost function composes step-wise objective vectors \vec{f} that evaluate the quality of each step, $\Phi : \mathbb{R}^{|\vec{f}| \times n} \rightarrow \mathbb{R}^{|\vec{f}|}$ aggregates objectives across steps (e.g., sum or max), and E maps the result to a scalar (e.g., weighted sum). C_{prec} , C_{kin} , C_{col} represent part precedence, kinematic, and collision constraints respectively. Please refer to App. B for detailed constraint formulation.

Solving for feasible or even optimal solutions in a joint manner is intractable. We present a hierarchical approach to decompose it into simpler subproblems for efficient computation with optimality guarantees under assumptions (A1)-(A5). The complete pseudocode can be found in App. C.

3.1 Part Precedence Planning

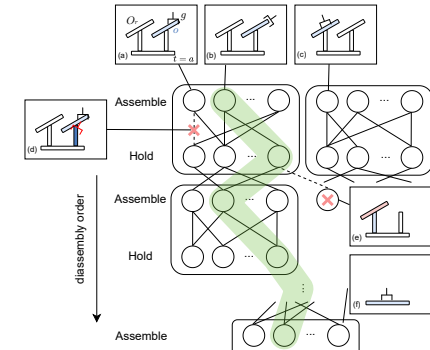
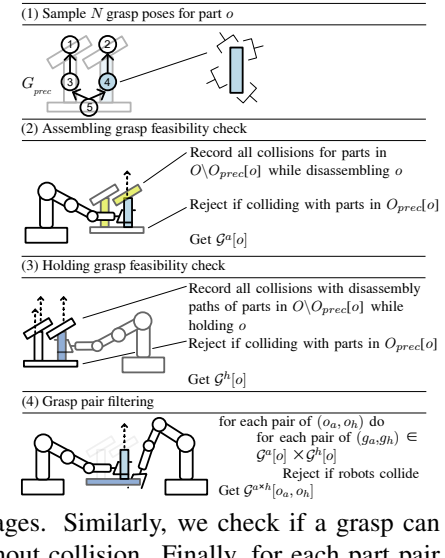
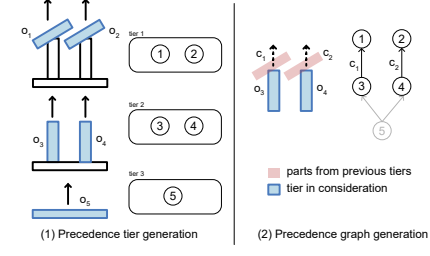
To evaluate constraint C_{prec} , we propose an algorithm to determine the complete precedence relationships for assembling all parts O . First, we define precedence tier as a group of parts that can be removed independently of one another. Tiers are ordered so that parts in earlier tiers must be disassembled before those in later ones. To iteratively construct all tiers, we use a physics-based motion planner [10] to find all parts that can be disassembled without interfering with the rest, which are grouped into the current tier. We then remove these parts and repeat the process on the remaining assembly until each part is assigned to a tier. Next, we build a precedence graph G_{prec} that encodes the minimal set of ordering constraints that any collision-free assembly sequence must follow. Each node in G_{prec} is a part, and a directed edge $o_i \rightarrow o_j$ means that o_i must be assembled before o_j because o_j blocks the (dis)assembly path τ_{o_i} planned during tier generation. For each part o , we define its precedence set $O_{\text{prec}}[o] = \{o' | (o' \rightarrow o) \in G_{\text{prec}}\}$ as all parts that must be assembled before it.

3.2 Dual-Arm Grasp Filtering

We aim to identify valid grasp pairs $\mathcal{G}^{a \times h}[o_a, o_h]$ for each assembly-hold part pair (o_a, o_h) which support insertion and holding without colliding with preceding parts of o_a and o_h . Since searching the full 6-DoF space is infeasible, we assume feasible grasps exist in a dense, finite set of grasps, see (A5). Because each grasp must be checked for collisions with the current subassembly $\psi_{1:i}$, doing this online results in repeated and expensive checks against many part combinations. To speed up, we precompute valid grasps offline by sampling grasp candidates and performing parallelized inverse kinematics (IK) and collision checks for both arms. In practice, we simulate the robot following the part’s disassembly path τ_o and reject it if the motion collides with the precedence set $O_{\text{prec}}[o]$. All collisions and motions are recorded for reuse in later stages. Similarly, we check if a grasp can securely hold a part while disassembling other parts without collision. Finally, for each part pair (o_a, o_h) , we filter feasible grasps (g_a, g_h) by checking interarm collisions under computed IK.

3.3 Dual-Arm Sequence-Grasp Optimization

With all valid grasps computed, we now solve for the optimal sequence ϕ^* and grasps σ^* in Eq. 2. We formulate this as a state-space search problem and construct a directed state tree T_G , where each node represents a partial assembly state $s = (t, O_r, o, g)$ consisting of robot task t (assemble or hold), assembled parts O_r , part being grasped o , and grasp pose g . Starting from root nodes (complete assembly), we recursively expand the tree by alternating between assembling and holding, pruning states that violate constraints. Valid transitions must also respect precomputed grasp feasibility between successive steps. All collision and motion feasibility checks are reused from the earlier filtering stage. Each transition is scored by a grasp stability vector \vec{f} , capturing objectives such as supportiveness of the held part, frequency of grasp switches, torque stability, and contact area, which are designed to be lightweight yet effective for downstream control. We apply dynamic programming (DP) to propagate the best cumulative scores through the tree and identify the optimal solution. Please find more details in App. C.3.



3.4 Grasp-Aware Pickup Fixture Generation

For precise pickup, we develop a software-hardware co-design approach to automatically generate a fixture that stabilizes and orients each part for top-down pickup, based on planned grasps in Sec. 3.3. This removes the need for reorientation or regrasping between pickup and assembly, allowing the system to focus on the core assembly challenges. We first determine each part’s pickup pose in the world frame, with its orientation defined by the rotation from the assembly grasp to a top-down grasp. We then compute pickup positions by packing parts on the XY plane to avoid collisions between parts and the gripper. To reduce material usage and workspace area, we model this as a bin-packing problem and solve it with an iterative algorithm that alternates between packing, collision checking, and resolution. Finally, we generate the fixture by creating mold cavities based on the part geometries and poses, ensuring stable placement. See details in App. C.4 and examples in Fig. 3.

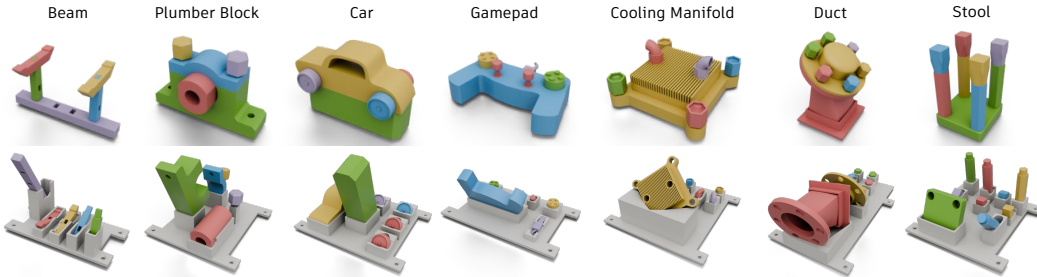


Figure 3: Top: benchmark assemblies. Bottom: the auto-generated pickup fixtures in Sec. 3.4.

3.5 Motion Planning for Transit and Transfer

Finally, RRT-Connect [45] plans for all remaining transit and transfer motions, i.e., $\tau_{a,i}^f, \tau_{a,i}^g, \tau_{h,i}^f$, which can be parallelized since all start and goal states of motions are provided from earlier stages.

4 Learning General Single-Step Assembly Policy

Once the full assembly plan is computed, the next challenge is to track it reliably in the real world. We use a hybrid controller that alternates between tracking the pre-planned transit and transfer motions, and an RL-based reactive controller for contact-rich assembly steps. The controller must generalize across variations in object geometry, grasp poses, and assembly directions. To this end, we design a lightweight yet highly effective RL framework for training a generalist assembly policy. Given a pre-planned insertion path τ_o , our goal is to guide the part from its noisy initial pose $\hat{\tau}_o[0]$ to the goal pose $\hat{\tau}_o[1]$, accounting for uncertainty in grasp and mating part geometry. We frame this as a Markov decision process (MDP) and learn a policy $\pi : \mathcal{O} \rightarrow \mathbb{P}(\mathcal{A})$ that maximizes expected rewards over time $\mathbb{E}_{\pi}[\sum_{t=0}^{T-1} \gamma^t r(s_t)]$. We use proximal policy optimization (PPO) [46] to train a stochastic policy in simulation, which is then transferred to the real world without additional fine-tuning.

4.1 Path-Centric Coordinate Transformation

Humans naturally reuse the same assembly skills across different objects, regardless of their poses or motions. We emulate this ability by designing a problem space transformation [47] with SE(3)-equivariance, which maps all straight-line assembly motions in the world frame into equivalent top-down insertions in the task frame, allowing the RL agent to perceive them in a unified way.

Formally speaking, given an assembly path τ with a pre-assembly position p_d and the assembled position p_a , we define a path-centric transformation \mathbf{T} conditioned on τ such that $\mathbf{T}(p_d) = (0, 0, 0)$ and $\mathbf{T}(p_d) - \mathbf{T}(p_a) = (0, 0, \|p_d - p_a\|)$. Thus, the agent’s observation is the transformed position of the part being assembled (under unknown noise), and its action is the transformed delta position, i.e., the ideal position change in the path-centric frame. Thanks to equivariance, the agent only needs to learn top-down insertions and can omit orientation from both observations and actions,

simplifying the learning setup. We use a task-space impedance (TSI) controller to enable smooth and compliant insertions, with impedance gains similarly transformed into the path-centric frame to maintain consistent behavior across different assembly directions. This design ensures that the observation and action spaces are minimal yet essential, facilitating generalizability among different assembly tasks, and is transferable to different robot arms and end effectors.

4.2 Plan-Guided Residual Action

We find that guidance from the planned open-loop action helps learning by injecting prior knowledge about the coarse assembly direction. Thus, we adopt the idea of residual action [48, 31] in RL, where the policy outputs only the corrective action on top of the open-loop action, allowing the policy to focus on refining the assembly rather than learning the full assembly behavior. In practice, residual action warm-starts policy learning and typically leads to faster and better convergence.

4.3 Minimalist Reward Design and Sim-to-Real Transfer

Surprisingly, our insertion reward is simply the negative L2 distance from the current part position to the goal position. This form is dense and sufficient enough for learning effective local insertion policies as our initial state is the pre-assembled pose given by the planner, which is already in the proximity of the goal thus does not require expensive exploration or complex reward engineering.

Due to the sim-to-real gap from misaligned dynamics, we adopt 1) domain randomization with 3mm-noised initialization on object pose during training and 2) Policy-Level Action Integrator (PLAI) [26] during deployment to ease the sim-to-real transfer of RL policies, which improves action consistency by incrementally applying policy outputs to the last desired state instead of the current state. PLAI applies policy actions as $s_{t+1}^d = s_t^d \oplus \Pi(o_t)$, where s_t^d represents the desired state at time t , $\Pi(o_t)$ is the policy action computed based on the current observation o_t , and \oplus denotes the composition operation, instead of the nominal approach $s_{t+1}^d = s_t \oplus \Pi(o_t)$ which is prone to error accumulation.

5 Experiments

5.1 Benchmark Suite and Experimental Setup

We develop a diverse benchmark suite spanning furniture, toys, and industrial equipment, which includes **beam** (5 parts), **plumber block** (5 parts), **car** (6 parts), **gamepad** (6 parts), **cooling manifold** (7 parts), **duct** (8 parts), and **stool** (9 parts). These assemblies cover various geometries and connection types found in real-world applications, with both top-down and sideway insertions, and are feasible for dual-arm robots with parallel grippers. For planning in simulation, we demonstrate on several different robots, including Franka Emika Panda, UFactory xArm7, and UR5e with different grippers. We use Panda for systematic evaluations of policy training and real-world execution. See more details on the experimental setup and hyper-parameters in App. D.

5.2 Planning Multi-Step Assembly in Simulation

Efficiency: Table 1 shows the breakdown of planning time by stages for different assemblies. Our overall speed is on the order of minutes to solve for optimal plans given efficient parallelization.

Optimality: Table 2 shows the objective scores of optimized sequences surpassing the random ones by a large margin with priorities from f_1 to f_4 (see App. C.3 for details on the score definitions).

Generality: Please see App. A for visual demonstrations of planning with different robot arms (Panda, xArm7, UR5e) and grippers. Our planning framework is general to any given hardware.

5.3 Learning Single-Step Assembly in Simulation

We use Isaac Gym [49] for training RL policies and performing simulation evaluations, with the PPO code from RL Games [50]. Table 3 presents the average % of successful steps for assembling our

Table 1: Planning runtime breakdown of each assembly. Stages marked with * are parallelized, while others have yet to be parallelized.

Assembly	Runtime (s)					
	Prec*	Grasp*	Seq	Fixture	Motion	Total
Beam	19.7	35.7	0.2	1.7	115.9	173.2
Plumber	21.6	31.8	12.6	0.9	118.9	185.7
Car	23.4	52.9	0.9	1.9	127.4	206.4
Gamepad	22.2	37.2	4.5	3.6	117.4	184.8
Manifold	20.9	162.7	5.2	1.9	149.6	340.4
Duct	93.9	102.3	208.1	2.5	185.9	592.7
Stool	57.2	109.1	8.0	4.0	324.5	502.7

Table 2: Objective comparisons between optimal and random sequences. Higher is better for f_1, f_4 ; lower is better for f_2, f_3 .

Assembly	Objective Values (Optimal / Random)			
	$f_1 \uparrow$	$f_2 \downarrow$	$f_3 \downarrow$	$f_4 \uparrow$
Beam	4.00 / 0.88	4.00 / 0.88	0.48 / 0.39	119.8 / 6.8
Plumber	4.00 / 1.27	2.00 / 1.79	0.18 / 0.33	293.0 / 93.4
Car	4.00 / 1.72	1.00 / 1.64	0.21 / 0.94	140.6 / 35.2
Gamepad	5.00 / 1.76	1.00 / 1.56	1.40 / 0.63	428.6 / 52.1
Manifold	6.00 / 2.62	1.00 / 2.17	0.18 / 0.69	12.5 / 18.7
Duct	6.00 / 3.00	1.00 / 2.88	0.09 / 0.39	536.0 / 101.3
Stool	8.00 / 3.43	6.00 / 3.24	0.03 / 0.54	322.2 / 87.9

Table 3: % of successful steps without intervention in simulation evaluations.

Method	% of Successful Steps without Intervention (Simulation)						
	Beam	Plumber Block	Car	Gamepad	Cooling Manifold	Duct	Stool
Open-Loop Tracking	21.48	24.22	2.34	2.34	3.91	18.75	0.00
Part Specialist Policy (PS)	98.63	84.08	90.82	87.60	94.63	100.00	78.91
Assembly Specialist Policy (AS)	99.12	97.46	70.12	88.87	95.02	96.58	76.66
Assembly Generalist Policy (AG)	98.83	81.64	60.55	71.48	89.06	89.84	58.59

benchmark assemblies in simulation across 1024 random trials using different methods: 1) **Open-Loop Tracking**: A baseline that strictly follows the pre-planned path without feedback correction. 2) **Part Specialist Policy (PS)**: Policies trained on individual pairs of parts. 3) **Assembly Specialist Policy (AS)**: Policies trained on all parts within a single assembly. 4) **Assembly Generalist Policy (AG)**: Policies trained on all parts from all assemblies in our suite, aiming for broad generalization.

The results show that open-loop tracking exhibits the lowest success rates across all assemblies, indicating its limitations in handling uncertainties and variations. The AS policy demonstrates competitive performance as the PS policy, suggesting that a shared policy across different parts in an assembly can generalize well. It may sacrifice some part-specific optimization, but can transfer the knowledge between similar parts. The AG policy, while slightly less effective than the other RL counterparts, still demonstrates robust performance, suggesting that learning a single shared policy across different assemblies is promising, given the equivariant representations. Furthermore, the success rates vary across different assemblies, with simpler assemblies like the Beam and Cooling Manifold achieving higher performance across all methods, while more complex assemblies such as the Gamepad and Stool exhibit lower success rates due to their intricate geometries and constraints.

5.4 Executing Multi-Step Assembly in Real World

Table 4 shows the % of successful steps on benchmark assemblies evaluated in the real world (step-wise statistics), and Table 5 shows the multi-step cumulative success rates with 0/1/2 total interventions for failure recovery (overall statistics). All numbers are averaged across three complete multi-step real experiments, which translate to thousands of total assembly steps. We deploy stochastic policies with state-based success detection and allow up to three trials per step until success. For qualitative results on real-world multi-step executions, please refer to Fig. 1 and App. A.

Ours: We use both AS and AG policies for real-world comparisons. For AG, we perform out-of-distribution (OOD) evaluations by training 7 generalist policies, where each one is trained on the other 6 benchmark assemblies (excluding the test assembly). Remarkably, these OOD generalist policies still achieved comparable performance to specialist policies trained directly on the test assembly, which indicates that through our approach, insertion strategies learned from a diverse set of assemblies can effectively transfer to novel, unseen assemblies.

Baseline: Since Fabrica is the first to assemble general multi-part objects with only CAD input, identifying a comparable SOTA baseline is challenging. The closest work is ASAP [11], which performs single-arm kinematic feasibility search without sequence/grasp optimization or closed-loop control. To compare, we adapted it by planning with dual-arm and adding our RL policy. Without optimized part sequencing and grasping, ASAP performed substantially worse, often struggling even with two interventions, which emphasizes the contributions of our planning optimizations.

Table 4: % of successful steps without intervention in real-world evaluations.

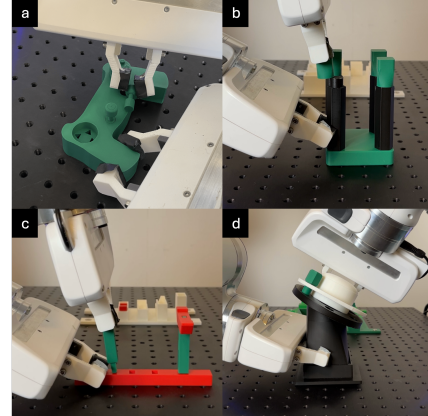
Method		% of Successful Steps without Intervention (Real World)							
		Beam	Plumber Block	Car	Gamepad	Cooling Manifold	Duct	Stool	Overall
Ours	AS AG (OOD)	75 <u>67</u>	83 <u>75</u>	80 <u>93</u>	87 <u>80</u>	72 <u>72</u>	71 <u>81</u>	92 <u>92</u>	80 <u>80</u>
Baseline	ASAP (Adapted) Open-Loop Tracking	50 42	42 25	67 20	33 20	55 17	52 14	75 <u>21</u>	55 23
Ablation	w/o Part Seq Optim w/o Grasp Optim w/o Path-Centric Transform	75 42 <u>67</u>	75 83 67	73 47 20	40 60 53	61 67 78	71 <u>67</u> 38	92 <u>75</u> 92	71 64 61

Table 5: Multi-step cumulative success rate with 0/1/2 interventions in real-world evaluations.

Method		Multi-Step Cumulative Success Rate with 0/1/2 Interventions (%) (Real World)							
		Beam	Plumber Block	Car	Gamepad	Cooling Manifold	Duct	Stool	Overall
Ours	AS AG (OOD)	0/100/100 0/ 67/100	33/100/100 0/100/100	0/100/100 67/100/100	33/100/100 0/100/100	0/ 67/ 67 0/ 33/100	0/ 0/100 0/ 67/100	33/100/100 33/100/100	15/ 81/ 95 <u>10/ 81/100</u>
Baseline	ASAP (Adapted) Open-Loop Tracking	0/ 0/100 0/ 0/ 67	0/ 0/ 67 0/ 0/ 33	0/ 33/100 0/ 0/ 0	0/ 0/ 0 0/ 0/ 0	0/ 0/ 33 0/ 0/ 0	0/ 0/ 0 0/ 0/ 0	0/ 0/ 0 0/ 0/ 0	0/ 5/ 57 0/ 0/ 14
Ablation	w/o Part Seq Optim w/o Grasp Optim w/o Path-Centric Transform	0/100/100 0/ 0/ 67 0/ 67/100	33/ 67/100 33/100/100 0/ 67/100	0/ 67/100 0/ 0/ 33 0/ 0/ 0	0/ 0/ 0 0/ 0/ 100 0/ 0/ 67	0/ 0/ 67 0/ 0/100 0/ 67/100	0/ 0/100 0/ 0/ 67 0/ 0/ 0	33/100/100 0/ 0/100 33/100/100	10/ 48/ 81 5/ 14/ 81 5/ 43/ 67

Ablation: To understand how much optimizing part sequences and grasps helps, we conduct ablation studies on our method by removing those optimizations respectively. We observed that suboptimal sequencing often caused instability due to inadequate support of critical neighboring parts and more part drifts due to unnecessary re-grasps. Meanwhile, suboptimal grasp selection frequently caused part slippage due to insufficient contact area or inadequate resistance to external torques. Thus, our planner inherently accounts for control-level uncertainties, and results demonstrate that selecting effective part sequences and grasps significantly enhances assembly reliability. For control, we observed that our path-centric transformation is crucial for generalizing across varying assembly directions. Policies trained without it perform significantly worse when multiple directions are involved. For more studies on the effects of path-centric transformation and residual actions introduced in Sec 4, and success increase w.r.t. the number of trials per step, please see App. E.

Failures: We observed a noticeable gap between simulation and real-world performances. Thus, we present a detailed analysis of common failure cases shown in the right figure: a) Small parts slip between gripper pads during insertion attempts; b) Cumulative error accrued during the assembly of large assemblies increases the displacement error of final part insertions; c) The holding gripper is not modeled during RL training, causing unexpected part obstructions in the real world; d) Unstabilized parts shift previously assembled parts during insertion. We assume a 3mm noise in simulation given that the base part is stably held. However, many sources of real-world error lead to much more significant errors than simulated, which are non-trivial challenges for future work. Due to these failures, all methods achieve near-zero multi-step success rates without intervention due to inherently challenging steps causing consistent failures. However, with minimal interventions, our method significantly outperforms others, reaching 81% success with one intervention and 95% with two.



6 Conclusion

We presented Fabrica, a dual-arm robotic system that innovates and integrates global hierarchical planning with local generalist policy learning for autonomous multi-part assembly. To support reproducible and rigorous evaluation, we introduced a comprehensive benchmark suite covering diverse multi-part assemblies. Fabrica is the first to demonstrate robust and generalizable performance across a wide range of real-world assembly tasks. We discuss limitations and future work in Sec 7.

7 Limitations and Future Work

While Fabrica shows promising results for autonomous multipart assembly, there remain several limitations and opportunities for future extension.

Assumptions: The assumptions we make in this problem formulation are the following:

- (A1) *Insertion-only assembly*: We assume that the mating between two parts only involves an insertion motion, without requiring skills like screwing or sliding.
- (A2) *No subassembly reorientation*: The final assembled positions of all parts are assumed to be given and fixed during the assembly process. This means that no further movement or re-orientation is allowed once a part is assembled.
- (A3) *Monotonic assembly*: Each part is only moved once, without considering regrasps, in-hand manipulation, or handovers.
- (A4) *No force and torque constraints for the robots*: We assume all parts are light compared to the robot payload.
- (A5) *A finite grasp set for each part*: $\forall g \in \sigma, g \in \mathcal{G}[o], |\mathcal{G}[o]| = N$, where $\mathcal{G}[o]$ can be computed by any grasp generator.

The above assumptions leave areas such as handling heavier parts, managing grasp slippage, and performing other operations such as screwing or sliding unaddressed. Incorporating these capabilities would significantly improve the robustness and applicability of Fabrica in more complex and diverse assembly tasks.

Dexterity: Moreover, the current setup enforces a fixed part pose once assembled. This is in contrast with the more dexterous human assembly behavior, where one would constantly reorient the partial assembly so that the parts are easily reachable. However, allowing reorientation would introduce additional planning overhead and more uncertainty for control due to potential subassembly instability. Addressing it will enable a more dexterous robotic system that can handle large assemblies that are beyond the reach of the current system, e.g., a large tabletop with parts on both sides.

Hardware capability: Compared to the existing multipart assembly dataset with thousands of objects [10], our current benchmark is limited in its size and diversity. This is because we want to ensure that the benchmark tasks are achievable by commonly used parallel grippers, but these grippers have a limited grasp width and thus cannot establish stable antipodal grasps for parts with large and complex geometries. However, to broaden the assembly capability, we can envision either a multi-finger hand or a multi-tool system in which the robots can switch specialized grippers according to the part geometry, and our planning and control system could be adapted to this setting.

Practical integration A key practical limitation of the current setup is sensitivity to localization calibration of the two arms. Each arm’s ability to reach commanded poses with millimeter-level precision depends on the fidelity of its own kinematic model and calibration. Small errors in joint encoder offsets, link dimensions, or tool center point definition can cause systematic deviations between the planned and actual end-effector poses. Regular in-situ calibration against a reference artifact or workspace-specific pose verification could mitigate this issue, but such steps introduce additional setup and maintenance effort not yet addressed in the present system. In addition, repeated insertions and extractions can cause gradual wear of the pickup fixture, leading to deviations from the planned motions. This sensitivity is amplified by the tight tolerances inherent to the assembly, where even sub-millimeter shifts can result in failures. Incorporating perception capabilities, as illustrated below, could enable the system to detect and adapt to such deviations in real time, compensating for both calibration errors and tolerance-induced misalignments.

Perception: Integrating vision systems for alignment feedback could greatly improve the accuracy and adaptability of the assembly process. By incorporating perception, the system could enable direct bin-picking, allowing it to grasp parts from random, unknown initial poses instead of requiring

a specialized pickup fixture. However, bin-picking remains a well-known challenge in industry, particularly in terms of robustness and generalizability across arbitrary part geometries and physical properties. Addressing these challenges requires substantial research and development efforts, but would significantly expand the practical applications of our approach.

Data collection: Collecting real-world assembly data is challenging due to the task’s long-horizon, contact-rich nature and the high cost of acquiring or fabricating diverse assembly assets. Fabrica addresses these barriers by enabling fully autonomous data collection in simulation and requiring only minimal human intervention in the real world. In future work, we aim to leverage this capability to generate large-scale, diverse datasets of assembly trajectories. These datasets can facilitate broader research in generalizable policy learning, sim-to-real transfer, and foundation models for robotic manipulation. Moreover, because assembly is one of the most constrained and demanding manipulation tasks, learning from assembly data has the potential to positively transfer to a wide range of general-purpose manipulation skills.

Acknowledgments

This work is funded by Autodesk, and in part by NSF 1846368 & 2313076. Yijiang Huang is supported by the SNSF Ambizione program. The authors would like to thank Bingjie Tang and Lars Ankle for insightful discussions during the RL environment setup, Xiang Zhang and Yotto Koga for valuable advice on the early physical setup, the members of Ted Adelson’s lab at MIT for their support with the physical Panda robot, and the MIT SuperCloud and Lincoln Laboratory for HPC resources.

References

- [1] J. Xu, S. Kim, T. Chen, A. R. Garcia, P. Agrawal, W. Matusik, and S. Sueda. Efficient tactile simulation with differentiability for robotic manipulation. In *6th Annual Conference on Robot Learning*, 2022.
- [2] X. Zhang, M. Tomizuka, and H. Li. Bridging the sim-to-real gap with dynamic compliance tuning for industrial insertion. In *ICRA*, 2024.
- [3] B. Tang, I. Akinola, J. Xu, B. Wen, A. Handa, K. Van Wyk, D. Fox, G. S. Sukhatme, F. Ramos, and Y. Narang. Automate: Specialist and generalist assembly policies over diverse geometries. In *Robotics: Science and Systems*, 2024.
- [4] D. Halperin, J.-C. Latombe, and R. H. Wilson. A general framework for assembly planning: The motion space approach. *Algorithmica*, 26(3):577–601, 2000.
- [5] S. Sundaram, I. Remmler, and N. M. Amato. Disassembly sequencing using a motion planning approach. In *Proceedings 2001 ICRA. IEEE International Conference on Robotics and Automation (Cat. No. 01CH37164)*, volume 2, pages 1475–1480. IEEE, 2001.
- [6] D. T. Le, J. Cortés, and T. Siméon. A path planning approach to (dis) assembly sequencing. In *2009 IEEE International Conference on Automation Science and Engineering*, pages 286–291. IEEE, 2009.
- [7] X. Zhang, R. Belfer, P. G. Kry, and E. Vouga. C-space tunnel discovery for puzzle path planning. *ACM Transactions on Graphics (TOG)*, 39(4):104–1, 2020.
- [8] N. Funk, G. Chalvatzaki, B. Belousov, and J. Peters. Learn2assemble with structured representations and search for robotic architectural construction. In *Conference on Robot Learning*, pages 1401–1411. PMLR, 2022.
- [9] S. K. S. Ghasemipour, S. Kataoka, B. David, D. Freeman, S. S. Gu, and I. Mordatch. Blocks assemble! learning to assemble with large-scale structured reinforcement learning. In *International Conference on Machine Learning*, pages 7435–7469. PMLR, 2022.
- [10] Y. Tian, J. Xu, Y. Li, J. Luo, S. Sueda, H. Li, K. D. Willis, and W. Matusik. Assemble them all: Physics-based planning for generalizable assembly by disassembly. *ACM Transactions on Graphics (TOG)*, 41(6):1–11, 2022.
- [11] Y. Tian, K. D. Willis, B. Al Omari, J. Luo, P. Ma, Y. Li, F. Javid, E. Gu, J. Jacob, S. Sueda, et al. Asap: Automated sequence planning for complex robotic assembly with physical feasibility. In *2024 IEEE International Conference on Robotics and Automation (ICRA)*, pages 4380–4386. IEEE, 2024.
- [12] I. Rodríguez, K. Nottensteiner, D. Leidner, M. Kaßecker, F. Stulp, and A. Albu-Schäffer. Iteratively refined feasibility checks in robotic assembly sequence planning. *IEEE Robotics and Automation Letters*, 4(2):1416–1423, 2019.
- [13] X. Zhu, D. K. Jha, D. Romeres, L. Sun, M. Tomizuka, and A. Cherian. Multi-level reasoning for robotic assembly: From sequence inference to contact selection. In *2024 IEEE International Conference on Robotics and Automation (ICRA)*, pages 816–823. IEEE, 2024.

- [14] F. Suárez-Ruiz, X. Zhou, and Q.-C. Pham. Can robots assemble an ikea chair? *Science Robotics*, 3(17):eaat6385, 2018.
- [15] L. Nägele, A. Hoffmann, A. Schierl, and W. Reif. Legobot: Automated planning for coordinated multi-robot assembly of lego structures. In *2020 IEEE/RSJ International Conference on Intelligent Robots and Systems (IROS)*, pages 9088–9095. IEEE, 2020.
- [16] Y. Huang, C. R. Garrett, I. Ting, S. Parascho, and C. T. Mueller. Robotic additive construction of bar structures: Unified sequence and motion planning. *Construction Robotics*, 5:115–130, 2021.
- [17] Y. Huang, P. Y. V. Leung, C. Garrett, F. Gramazio, M. Kohler, and C. Mueller. The new analog: A protocol for linking design and construction intent with algorithmic planning for robotic assembly of complex structures. In *Proceedings of the 6th Annual ACM Symposium on Computational Fabrication*, pages 1–17, 2021.
- [18] Z. Wang, F. Kennel-Maushart, Y. Huang, B. Thomaszewski, and S. Coros. A temporal coherent topology optimization approach for assembly planning of bespoke frame structures. *ACM Transactions on Graphics (TOG)*, 42(4):1–13, 2023.
- [19] C.-J. Liang, S.-C. Kang, and M.-H. Lee. Ras: a robotic assembly system for steel structure erection and assembly. *International Journal of Intelligent Robotics and Applications*, 1:459–476, 2017.
- [20] K. Dörfler, T. Sandy, M. Gifthaler, F. Gramazio, M. Kohler, and J. Buchli. Mobile robotic brickwork: automation of a discrete robotic fabrication process using an autonomous mobile robot. *Robotic Fabrication in Architecture, Art and Design 2016*, pages 204–217, 2016.
- [21] A. A. Apolinarska, M. Pacher, H. Li, N. Cote, R. Pastrana, F. Gramazio, and M. Kohler. Robotic assembly of timber joints using reinforcement learning. *Automation in Construction*, 125:103569, 2021.
- [22] A. Kramberger, A. Kunic, I. Iturrate, C. Sloth, R. Naboni, and C. Schlette. Robotic assembly of timber structures in a human-robot collaboration setup. *Frontiers in Robotics and AI*, 8:768038, 2022.
- [23] G. Thomas, M. Chien, A. Tamar, J. A. Ojea, and P. Abbeel. Learning robotic assembly from cad. In *2018 IEEE International Conference on Robotics and Automation (ICRA)*, pages 3524–3531. IEEE, 2018.
- [24] Y. Fan, J. Luo, and M. Tomizuka. A learning framework for high precision industrial assembly. In *2019 International Conference on Robotics and Automation (ICRA)*, pages 811–817. IEEE, 2019.
- [25] Y. Narang, K. Storey, I. Akinola, M. Macklin, P. Reist, L. Wawrzyniak, Y. Guo, A. Mora-vanszky, G. State, M. Lu, et al. Factory: Fast contact for robotic assembly. *arXiv preprint arXiv:2205.03532*, 2022.
- [26] B. Tang, M. A. Lin, I. Akinola, A. Handa, G. S. Sukhatme, F. Ramos, D. Fox, and Y. Narang. Industreal: Transferring contact-rich assembly tasks from simulation to reality. *arXiv preprint arXiv:2305.17110*, 2023.
- [27] X. Zhang, C. Wang, L. Sun, Z. Wu, X. Zhu, and M. Tomizuka. Efficient sim-to-real transfer of contact-rich manipulation skills with online admittance residual learning. In *Conference on Robot Learning*, pages 1621–1639. PMLR, 2023.
- [28] J. Luo, Z. Hu, C. Xu, Y. L. Tan, J. Berg, A. Sharma, S. Schaal, C. Finn, A. Gupta, and S. Levine. Serl: A software suite for sample-efficient robotic reinforcement learning. *arXiv preprint arXiv:2401.16013*, 2024.

- [29] M. Noseworthy, B. Tang, B. Wen, A. Handa, N. Roy, D. Fox, F. Ramos, Y. Narang, and I. Akinola. Forge: Force-guided exploration for robust contact-rich manipulation under uncertainty. *arXiv preprint arXiv:2408.04587*, 2024.
- [30] L. Ankile, A. Simeonov, I. Shenfeld, and P. Agrawal. Juicer: Data-efficient imitation learning for robotic assembly. *arXiv*, 2024.
- [31] L. Ankile, A. Simeonov, I. Shenfeld, M. Torne, and P. Agrawal. From imitation to refinement – residual rl for precise assembly, 2024. URL <https://arxiv.org/abs/2407.16677>.
- [32] H. Huang, D. Wang, A. Tangri, R. Walters, and R. Platt. Leveraging symmetries in pick and place. *The International Journal of Robotics Research*, page 02783649231225775, 2024.
- [33] A. Simeonov, Y. Du, A. Tagliasacchi, J. B. Tenenbaum, A. Rodriguez, P. Agrawal, and V. Sitzmann. Neural descriptor fields: Se (3)-equivariant object representations for manipulation. In *2022 International Conference on Robotics and Automation (ICRA)*, pages 6394–6400. IEEE, 2022.
- [34] A. Simeonov, Y. Du, Y.-C. Lin, A. R. Garcia, L. P. Kaelbling, T. Lozano-Pérez, and P. Agrawal. Se (3)-equivariant relational rearrangement with neural descriptor fields. In *Conference on Robot Learning*, pages 835–846. PMLR, 2023.
- [35] J. Yang, C. Deng, J. Wu, R. Antonova, L. Guibas, and J. Bohg. Equivact: Sim (3)-equivariant visuomotor policies beyond rigid object manipulation. *arXiv preprint arXiv:2310.16050*, 2023.
- [36] D. Wang, S. Hart, D. Surovik, T. Kelestemur, H. Huang, H. Zhao, M. Yeatman, J. Wang, R. Walters, and R. Platt. Equivariant diffusion policy. *arXiv preprint arXiv:2407.01812*, 2024.
- [37] J. Seo, N. P. Prakash, X. Zhang, C. Wang, J. Choi, M. Tomizuka, and R. Horowitz. Contact-rich se (3)-equivariant robot manipulation task learning via geometric impedance control. *IEEE Robotics and Automation Letters*, 2023.
- [38] W. Lian, T. Kelch, D. Holz, A. Norton, and S. Schaal. Benchmarking off-the-shelf solutions to robotic assembly tasks. In *2021 IEEE/RSJ International Conference on Intelligent Robots and Systems (IROS)*, pages 1046–1053. IEEE, 2021.
- [39] L. Fan, Y. Zhu, J. Zhu, Z. Liu, O. Zeng, A. Gupta, J. Creus-Costa, S. Savarese, and L. Fei-Fei. Surreal: Open-source reinforcement learning framework and robot manipulation benchmark. In *Conference on robot learning*, pages 767–782. PMLR, 2018.
- [40] Y. Lee, E. S. Hu, and J. J. Lim. Ikea furniture assembly environment for long-horizon complex manipulation tasks. In *2021 ieee international conference on robotics and automation (icra)*, pages 6343–6349. IEEE, 2021.
- [41] M. Heo, Y. Lee, D. Lee, and J. J. Lim. Furniturebench: Reproducible real-world benchmark for long-horizon complex manipulation. In *Robotics: Science and Systems*, 2023.
- [42] J. Luo, C. Xu, F. Liu, L. Tan, Z. Lin, J. Wu, P. Abbeel, and S. Levine. Fmb: a functional manipulation benchmark for generalizable robotic learning. *arXiv preprint arXiv:2401.08553*, 2024.
- [43] R. Alami, J.-P. Laumond, and T. Siméon. Two manipulation planning algorithms. In *WAFR Proceedings of the workshop on Algorithmic foundations of robotics*, pages 109–125. AK Peters, Ltd. Natick, MA, USA, 1994.
- [44] T. Siméon, J.-P. Laumond, J. Cortés, and A. Sahbani. Manipulation planning with probabilistic roadmaps. *The International Journal of Robotics Research*, 23(7-8):729–746, 2004.

- [45] J. J. Kuffner and S. M. LaValle. Rrt-connect: An efficient approach to single-query path planning. In *Proceedings 2000 ICRA. Millennium Conference. IEEE International Conference on Robotics and Automation. Symposia Proceedings (Cat. No. 00CH37065)*, volume 2, pages 995–1001. IEEE, 2000.
- [46] J. Schulman, F. Wolski, P. Dhariwal, A. Radford, and O. Klimov. Proximal policy optimization algorithms. *arXiv preprint arXiv:1707.06347*, 2017.
- [47] K. Doshi, M. Bagatella, and S. Coros. Problem space transformations for generalisation in behavioural cloning. *arXiv preprint arXiv:2411.04056*, 2024.
- [48] T. Silver, K. Allen, J. Tenenbaum, and L. Kaelbling. Residual policy learning. *arXiv preprint arXiv:1812.06298*, 2018.
- [49] V. Makoviychuk, L. Wawrzyniak, Y. Guo, M. Lu, K. Storey, M. Macklin, D. Hoeller, N. Rudin, A. Allshire, A. Handa, and G. State. Isaac gym: High performance gpu-based physics simulation for robot learning, 2021.
- [50] D. Makoviichuk and V. Makoviychuk. rl-games: A high-performance framework for reinforcement learning. https://github.com/Denys88/rl_games, May 2021.
- [51] A. Lodi, S. Martello, and M. Monaci. Two-dimensional packing problems: A survey. *European journal of operational research*, 141(2):241–252, 2002.
- [52] J. Jylänki. A thousand ways to pack the bin-a practical approach to two-dimensional rectangle bin packing, 2010. URL <https://raw.githubusercontent.com/juj/RectangleBinPack/master/RectangleBinPack.pdf>.